

Coprime array-based robust beamforming using covariance matrix reconstruction technique

Ke Liu^{1*} and Yimin D. Zhang²

¹ College of Automation, Harbin Engineering University, Harbin 150001, China

² Department of Electrical and Computer Engineering, Temple University, Philadelphia, PA 19122, USA

* E-mail: liuke_heu@163.com

Abstract: A novel robust adaptive beamforming algorithm based on coprime array is proposed in this paper. First, we exploit the virtual array structure of coprime coarray to construct two subspaces. The first subspace is obtained from the covariance matrix of the virtual uniform linear array (ULA). The second one is got by integrating spatial spectrum over each angular sector of signal. Then, by using a closed-form expression of projection-based approach, the steering vectors (SVs) of signals are estimated from the intersection of the two subspaces. Moreover, according to the covariance fitting theory, the power associated with the desired signal, interference signals and noise is obtained from the virtual sample covariance matrix. In addition, to reconstruct interference-plus-noise covariance matrix (INCM), the maximum correlation principle is used to transfer the virtual SVs of signals to real ones corresponding to a physical array. Finally, with the estimated the SV of the desired signal and the INCM, the proposed robust algorithm is devised. Simulation results demonstrate the superiority and effectiveness of the proposed algorithm.

1 Introduction

To enhance the directional gain of the desired signal (DS) and suppress interference signals, adaptive beamforming approaches are widely applied in various applications [1]-[3], such as wireless communications, radar, radio astronomy and medical imaging. Provided that the steering vector (SV) of the DS and the covariance matrix are accurately known, the traditional minimum variance distortionless response (MVDR) beamformer [4] achieves excellent performance. However, when the assumed DS direction has a mismatch or the covariance matrix contains the desired signal component, the MVDR beamformer can cause severe performance degradation. To overcome this shortcoming, a number of approaches have been developed to improve the robustness of beamformer in the past several decades. These approaches can be divided into the following two major categories: non-reconstruction approaches and reconstruction approaches. The former directly processes the sample covariance matrix (SCM) without a reconstruction operation. Such approaches include worst case approach [5], SV-estimation-based approaches [6], [7], and diagonal loading approaches [8], [9]. However, these methods cannot achieve near-optimal performance due to the self-nulling issue of the DS as a result of utilizing the sample covariance matrix.

As its name implies, reconstruction approaches [10]-[12] contain a key step of the SCM reconstruction corresponding to the interference signals. Compared with the non-reconstruction approaches, the reconstruction approaches generally yield an improved performance, which can be explained as follows. Recalling that the weight vector of the adaptive MVDR beamformer is a function of the INCM and the SV of the DS. By removing the DS component from the SCM, the self-nulling phenomenon of the DS is avoided. On the other hand, to avoid the look direction mismatch of the DS, the SV of the DS is accurately estimated by using certain optimization method. Hence, the output signal-to-interference-plus-noise ratio (SINR) of the reconstruction-based algorithms can closely converge to the optimal solution. It is noted that, in the reconstruction-based approaches, the noise power, the SV and the power of the each interference signal affect the INCM reconstruction. As a result, for INCM-reconstruction-based methods, it becomes critical to guarantee the estimation accuracy of the SVs and the power of the

interference signals. Toward this end, subspace-based methods are attractive due to their simplicity and high efficiency. In [13], the DS SV and the INCM are estimated by subspace projection. However, the beamformer performance still tremendously degrades in presence of look direction errors of the DS. In [14] [15], the maximum correlation principle is used to reconstruct the INCM, but the performance degrades when the input SNR is closed to the input interference-noise ratio (INR). The approach in [16] makes use of the *a priori* information about the angular sections of the signals and combines projection methods to obtain a more precise estimation of the INCM, but it has performance degradation with the increase of the interferer numbers.

Recently, the coprime-array-based signal processing approaches [17]-[28] attract a great attention since they can yield a higher estimated accuracy and a stronger interference suppression capability than the uniform linear array (ULA) counterpart when the same number of sensors are used. The main concept of the coprime array configuration is to use a pair of coprime sparse subarrays to compose a non-uniform linear array. By exploiting the difference coarray property of coprime coarray, a virtual ULA with more sensors than the number of physical ones is formulated. The equivalent received signals based on the virtual array are then utilized for parameter estimation. Compared to coprime-array-based DOA estimation which has attracted considerable interests, adaptive beamforming techniques based on coprime array are much less studied. Among the few references published in this area, reference [24] introduced a compressive matrix to transfer the steering vector of a virtual array to that of a physical array, based on which a coprime-array-based adaptive beamforming approach is developed. Such approach suffers from performance loss because of the reduced number of virtual sensors as a result of sparse sampling. In [25], based on the spatial spectrum estimated using a virtual array, the source directions and interference power are sequentially estimated and a coprime array adaptive beamformer is then constructed. In this case, the interference power obtained from Capon spectrum estimation may not be accurate, thus compromising the accuracy of the reconstructed interference covariance matrix and, subsequently, the adaptive beamformer. In references [26] and [27], a coprime array consisting of a pair of physical uniform linear subarrays is considered, and the signals vectors received in these subarrays are separately processed to

perform DOA and power estimations. In this approach, the number of sources that can be estimated is limited by that of the physical sensors of each uniform linear subarray. In reference [28], a sparse-reconstruction-based source estimation algorithm is proposed to simultaneously estimate the DOAs and power of the signals. Such approach can be directly extended to adaptive beamforming. It is noted that, however, it could encounter the off-grid issue and thus compromise the estimation performance.

Due to the fact above, in this paper, we propose a novel subspace approach to reconstruct INCM using a coprime array. The accurate estimations associated with the SVs and the power of signals are obtained by utilizing virtual aperture of the coprime array. Based on the vector correlation property, a connection can be built between the physical coprime array and the virtual ULA. To obtain a high-accuracy estimation of the physical array-based INCM and the DS SV, based on which, a novel robust adaptive beamformer is formulated. Simulation results demonstrate that the proposed coprime array adaptive beamforming algorithm is superior to existing approaches in terms of the output SINR. The key contribution of the proposed work lies in the accurate estimation of the INCM and the DS SV using virtual sensors by utilizing the larger aperture and the higher number of degrees of freedom of the virtual array. Such results enable the MVDR beamformer to achieve improved performance as compared to existing methods. In addition, we use a novel approach to estimate the signal steering vectors and the interference power based on the virtual array of the coprime array. To reconstruct the INCM in the physical coprime array, the signal steering vectors corresponding to the virtual array are mapped to those of the physical array based on the vector correlation property.

The rest of the paper is organized as follows. Section 2 introduces the array model based on coprime coarray. The proposed robust adaptive beamforming algorithm is presented in Section 3. In Section 4, simulation results are provided to illustrate the effectiveness of the proposed algorithm. Finally, conclusions are given in Section 5.

Notations: We use upper-case and lower-case to denote vector and matrices, respectively. In particular, \mathbf{I}_M denotes the $M \times M$ identity matrix. The superscripts $(\cdot)^T$ and $(\cdot)^H$ respectively imply transpose and conjugate transpose of a matrix or vector, and $(\cdot)^{-1}$ denotes matrix inversion operator. $\text{diag}(\cdot)$ and $\text{vec}(\cdot)$ represent diagonalization and vectorization operator, respectively. \otimes denotes the Kronecker product, and $E(\cdot)$ denotes the statistical expectation operator. $|\cdot|$ and $\|\cdot\|$ denote absolute value and Frobenius norm, respectively.

2 Signal model

Without loss of generality, we assume that M and N are a pair of coprime integers with $M < N$. Consider two uniform linear subarrays with sparse space and denote the unit inter-element spacing d to be half wavelength $\lambda/2$. For the first subarray, there are M sensors with inter-element spacing Nd , while the second subarray has N sensors with inter-element spacing Md . Assume that the first sensor of both subarrays shares the same position and is set as the reference. There are Q far-field uncorrelated narrowband signals impinging on the coprime array from directions $\{\theta_1, \theta_2, \dots, \theta_Q\}$. The first signal is considered as the DS. The received signal vector $\mathbf{x}(k) \in C^{M+N-1}$ is written as

$$\mathbf{x}(k) = \sum_{q=1}^Q \mathbf{a}(\theta_q) s_q(k) + \mathbf{n}(k) = \mathbf{A}\mathbf{s}(k) + \mathbf{n}(k), \quad (1)$$

where k is the snapshot index, $\mathbf{a}(\theta_q) = [1, e^{j\frac{2\pi p_2}{\lambda} \sin(\theta_q)}, \dots, e^{j\frac{2\pi p_{M+N-1}}{\lambda} \sin(\theta_q)}]^T$ is the SV of signal s_q ,

$$p_c \in \{Mnd|0 \leq n \leq N-1\} \cup \{Nmd|0 \leq m \leq M-1\} \quad (2)$$

$$c = 1, 2, \dots, M+N-1$$

denotes the position of the c th physical array sensor. In addition, $\mathbf{A} = [\mathbf{a}(\theta_1), \mathbf{a}(\theta_2), \dots, \mathbf{a}(\theta_Q)]$ is the steering matrix, and $\mathbf{n}(k)$ is the noise vector whose elements are assumed to be independent and identically distributed complex Gaussian random variables.

The output of the adaptive beamformer is expressed as

$$y(k) = \mathbf{w}^H \mathbf{x}(k), \quad (3)$$

where $\mathbf{w} \in C^{(M+N-1) \times 1}$ is the weight vector of the beamformer and is obtained by solving the following optimization problem

$$\min_{\mathbf{w}} \mathbf{w}^H \mathbf{R}_{i+n} \mathbf{w} \quad \text{subject to} \quad \mathbf{w}^H \mathbf{a}(\theta_1) = 1, \quad (4)$$

where $\mathbf{a}(\theta_1)$ is the SV of the DS and \mathbf{R}_{i+n} is the INCM. The closed-form solution of (4) is written as

$$\mathbf{w}_{\text{opt}} = \frac{\mathbf{R}_{i+n}^{-1} \mathbf{a}(\theta_1)}{\mathbf{a}^H(\theta_1) \mathbf{R}_{i+n}^{-1} \mathbf{a}(\theta_1)}, \quad (5)$$

which is the well-known MVDR beamformer [4].

In practice, \mathbf{R}_{i+n} is difficult to directly obtain and thus is usually replaced by the SCM

$$\hat{\mathbf{R}} = \frac{1}{L} \sum_{k=1}^L \mathbf{x}(k) \mathbf{x}^H(k) \quad (6)$$

from L snapshots. When the SCM is used in computing the beamformer weights, the SINR performance is not closely optimal. That is due to the fact that SCM contains the DS component which leads to the self-nulling phenomenon of DS. The interference-plus-noise covariance matrix reconstruction approach can be used to solve this issue efficiently.

3 Proposed algorithm

In order to implement the optimal closed-form solution of the MVDR beamformer depicted in (5), we need to obtain the INCM and the SV of the DS. The reconstruction of the INCM requires the SVs and the power of all interference signals as well as the noise power. Therefore, in total, we need three pieces of information, i.e., the SVs of all signals (including that of the DS and of the interference signals), the power of interference signals, and the noise power. In this paper, we develop a robust beamformer algorithm based on the high-accuracy estimation of these parameters. By utilizing a coprime array structure that offers a large virtual array aperture with the same number of physical sensors. First, we use the projection-based method in the context of coprime array to estimate the SVs of all signals. Then, by using the covariance fitting method, the power of the interference signals and noise is obtained. It is noted that the estimated SVs of all signals are based on the virtual array. The above estimated information is then used to reconstruct the INCM and the DS SV corresponding to the physical sensor array through the utilization of the maximum correlation principle. After obtaining the INCM and the DS SV associated with the physical array elements, the weight vector of the proposed adaptive beamformer is computed according to (5).

3.1 Coprime array-based steering vector estimation

To take the advantage of the virtual array aperture of a coprime coarray to obtain a high-precision estimation for the signal SV, we first vectorize the SCM $\hat{\mathbf{R}}$ as

$$\mathbf{z} = \text{vec}(\hat{\mathbf{R}}) = \tilde{\mathbf{A}}\mathbf{b} + \sigma_n^2 \tilde{\mathbf{I}}, \quad (7)$$

where $\tilde{\mathbf{A}} = [\tilde{\mathbf{a}}(\theta_1), \tilde{\mathbf{a}}(\theta_2), \dots, \tilde{\mathbf{a}}(\theta_Q)]$, $\tilde{\mathbf{a}}(\theta_q) = \mathbf{a}^*(\theta_q) \otimes \mathbf{a}(\theta_q)$, $\mathbf{b} = [\sigma_1^2, \sigma_2^2, \dots, \sigma_Q^2]$, and $\tilde{\mathbf{I}} = \text{vec}(\mathbf{I}_{M+N-1})$. It is easy to find that

the rank of the single-sample covariance matrix $\mathbf{R}_{zz} = \mathbf{z}\mathbf{z}^H$ is one. In other words, \mathbf{z} appears as a coherent single-snapshot received signal corresponding to a non-uniform virtual linear array. According to the difference coarray property of the coprime array, we choose the maximum consecutive lags of the virtual array from $-M_\xi$ to M_ξ to reconstruct \mathbf{z} . By deleting redundant virtual sensor entries and sorting them according to their positions, the rows of \mathbf{z} are identical to a consecutive virtual ULA. Rearranging the rows of \mathbf{z} [18] yields the new received signal vector \mathbf{z}_1 , which can be expressed as

$$\mathbf{z}_1 = \tilde{\mathbf{A}}_1 \mathbf{b} + \sigma_n^2 \tilde{\mathbf{I}}_1, \quad (8)$$

where $\tilde{\mathbf{A}}_1$ is the steering matrix of a virtual ULA with $2M_\xi + 1$ sensors located from $-M_\xi$ to M_ξ . $\tilde{\mathbf{I}}_1$ is an all-zero vector except one entry of 1 at the $(M_\xi + 1)$ th position.

To decorrelate the covariance matrix $\mathbf{R}_{z_1 z_1} = \mathbf{z}_1 \mathbf{z}_1^H$ and restore its rank, we construct the following Toeplitz matrix \mathbf{R}_1 [29], as \mathbf{R}_1 has an identical performance and a lower computational complexity as compared to the spatial smoothing matrix. Matrix \mathbf{R}_1 is expressed as

$$\mathbf{R}_1 = \begin{pmatrix} \langle \mathbf{z}_1 \rangle_0 & \langle \mathbf{z}_1 \rangle_{-1} & \cdots & \langle \mathbf{z}_1 \rangle_{-M_\xi} \\ \langle \mathbf{z}_1 \rangle_1 & \langle \mathbf{z}_1 \rangle_0 & \cdots & \langle \mathbf{z}_1 \rangle_{-M_\xi+1} \\ \vdots & \vdots & \ddots & \vdots \\ \langle \mathbf{z}_1 \rangle_{M_\xi} & \langle \mathbf{z}_1 \rangle_{M_\xi-1} & \cdots & \langle \mathbf{z}_1 \rangle_0 \end{pmatrix} \quad (9)$$

where $\langle \mathbf{z}_1 \rangle_v$ is the value corresponding to virtual sensor placed at vd . Then, the eigen-decomposition of matrix \mathbf{R}_1 is expressed as

$$\mathbf{R}_1 = \sum_{q=1}^{M_\xi+1} \lambda_q \tilde{\mathbf{e}}_q \tilde{\mathbf{e}}_q^H = \mathbf{E}_s \Lambda_s \mathbf{E}_s^H + \mathbf{E}_n \Lambda_n \mathbf{E}_n^H, \quad (10)$$

where $\lambda_q, q = 1, 2, \dots, M_\xi + 1$, are the eigenvalues of \mathbf{R}_1 in the descending order, and $\tilde{\mathbf{e}}_q$ are the corresponding eigen-vectors. $\mathbf{E}_s = [\tilde{\mathbf{e}}_1, \dots, \tilde{\mathbf{e}}_Q]$ spans the signal subspace and is made of Q dominant eigenvectors associated with the Q largest eigenvalues, whereas $\mathbf{E}_n = [\tilde{\mathbf{e}}_{Q+1}, \dots, \tilde{\mathbf{e}}_{M_\xi+1}]$ contains the remaining eigenvectors and spans the noise subspace.

In reference [30], a preprocessing step based on the projection of the assumed DS SV is used to reconstruct a more robust signal subspace. While this was applied only to the DS, we extend this concept to all signals. By noticing the fact that the *a priori* DOA information of each signal can be easily obtained using conventional low-resolution DOA estimation methods [12], [16], we utilize such information as a coarse DOA estimate for each signal and define an angular sector around it to obtain the corresponding signal subspace based on the approach described in [30]. Hence, for the j th signal $s_j, j = 1, 2, \dots, Q$, the eigenvectors associated with the large value by projecting the assumed SV $\tilde{\mathbf{a}}_j$ onto the $\tilde{\mathbf{e}}_q$, can be used to construct the signal subspace of s_j . To describe this process, a projection expression is introduced as

$$p_s(q) = |\tilde{\mathbf{e}}_q^H \tilde{\mathbf{a}}_j|^2, \quad q = 1, 2, \dots, M_\xi. \quad (11)$$

Then, we rearrange $p_s(q)$ in the descending order, i.e., $p_s(M_\xi) \geq p_s(M_\xi - 1) \geq \dots \geq p_s(1)$. Correspondingly, the columns of $\tilde{\mathbf{E}}_s$ are arranged as $[\tilde{\mathbf{e}}_{M_\xi}, \tilde{\mathbf{e}}_{M_\xi-1}, \dots, \tilde{\mathbf{e}}_1]$. We select Q dominant eigenvectors to form the signal subspace of s_j , expressed as

$$\mathbf{P}_{c1} = [\tilde{\mathbf{e}}_{M_\xi}, \tilde{\mathbf{e}}_{M_\xi-1}, \dots, \tilde{\mathbf{e}}_{M_\xi-Q}], \quad (12)$$

where Q is determined as the minimum integer value that ensures $[p_s(M_\xi) + p_s(M_\xi - 1) + \dots + p_s(M_\xi - Q)]/[2M_\xi + 1] > \rho$ with $\rho \in (0, 1)$ being a projection parameter. That is to say, the SV of the j th signal $\tilde{\mathbf{a}}_j$ lies in the subspace spanned by the columns of \mathbf{P}_{c1} , i.e.,

$$\tilde{\mathbf{a}}_j \in \Xi_s = [\tilde{\mathbf{a}} : \tilde{\mathbf{a}} = \mathbf{P}_{c1} \alpha_s], \quad (13)$$

where α_s is a coefficient vector and denotes the coefficients to the subspace vectors.

Considering the spatial domain property, we construct the following matrix

$$\mathbf{C}_j = \int_{\Theta_j} c(\theta) \tilde{\mathbf{a}}(\theta) \tilde{\mathbf{a}}^H(\theta) d\theta, \quad (14)$$

where $c(\theta)$ is the probability density function and could be set to either 1 [6] or $1/[\tilde{\mathbf{a}}^H(\theta) \tilde{\mathbf{R}}^{-1} \tilde{\mathbf{a}}(\theta)]$ [11], and $\Theta_j, j = 1, 2, \dots, Q$, denotes the angular sectors where the j th signal is located. Then, \mathbf{C}_j is eigendecomposed as

$$\mathbf{C}_j = \sum_{i=q}^{M_\xi+1} \beta_q \tilde{\mathbf{v}}_q \tilde{\mathbf{v}}_q^H = \mathbf{V}_s \Psi_s \mathbf{V}_s^H + \mathbf{V}_n \Psi_n \mathbf{V}_n^H, \quad (15)$$

where $\beta_q, q = 1, 2, \dots, M_\xi + 1$, are the eigenvalues of \mathbf{C}_j in the descending order, and $\tilde{\mathbf{v}}_q$ is the eigenvector corresponding to β_q . Similar to (10), \mathbf{V}_s contains H dominant eigenvector associated with the H largest eigenvalues, while \mathbf{V}_n contains the remaining $M_\xi + 1 - H$ eigenvectors. Following the method in [15], H is set as the minimum integer that satisfies $[\sum_{q=1}^H \beta_q] / [\sum_{q=1}^{M_\xi+1} \beta_q] > \varrho$, where $\varrho \in (0, 1)$ is a pre-determined parameter. Therefore, $\tilde{\mathbf{a}}_j$ lies in the subspace spanned by the columns of \mathbf{V}_s , i.e.,

$$\tilde{\mathbf{a}}_j \in \Xi_b = [\tilde{\mathbf{a}} : \tilde{\mathbf{a}} = \mathbf{V}_s \alpha_b], \quad (16)$$

where α_b is a coefficient vector similar to α_s .

To sum up, the SV of the j th signal $\tilde{\mathbf{a}}_j$ lies in the intersection of Ξ_s and Ξ_b , i.e., $\tilde{\mathbf{a}}_j \in \Xi_s \cap \Xi_b$. When using the iterative projection approach to obtain $\tilde{\mathbf{a}}_j$, the iteration equation is expressed as

$$\tilde{\mathbf{a}}_{j,h+1} = \mathbf{P}_1 \mathbf{P}_2 \tilde{\mathbf{a}}_{j,h}, \quad (17)$$

where the iterative start point is the assumed SV of $\tilde{\mathbf{a}}_j$, h is the iteration index, $\mathbf{P}_1 = \mathbf{P}_{c1} \mathbf{P}_{c1}^H$, and $\mathbf{P}_2 = \mathbf{V}_s \mathbf{V}_s^H$. When $h \rightarrow \infty$, $\tilde{\mathbf{a}}_{j,h}$ will converge to the actual SV of the j th signal [13] [15] [16]. By using the results in [31], we can prove that the maximum eigenvalue of $\mathbf{P}_1 \mathbf{P}_2$ is unity, i.e.,

$$\begin{aligned} \text{eig}_{max}(\mathbf{P}_1 \mathbf{P}_2) &\leq \max_{\mathbf{u}^H \mathbf{u} = 1} \mathbf{u}^H \mathbf{P}_1 \mathbf{u} \text{eig}_{max}(\mathbf{P}_2) \\ &= \max_{\mathbf{u}^H \mathbf{u} = 1} \frac{\mathbf{u}^H \mathbf{P}_1 \mathbf{u}}{\mathbf{u}^H \mathbf{u}} = \text{eig}_{max}(\mathbf{P}_1) = 1, \end{aligned} \quad (18)$$

where $\text{eig}_{max}(\cdot)$ denotes the maximum eigenvalue of a matrix. Therefore, considering the norm constraint, the SV of the j th signal $\tilde{\mathbf{a}}_j$ is obtained as

$$\hat{\mathbf{a}}_j = \sqrt{MN + 1} \Gamma[\mathbf{P}_1 \mathbf{P}_2], \quad j = 1, 2, \dots, Q, \quad (19)$$

where $\Gamma[\mathbf{P}_1 \mathbf{P}_2]$ denotes the eigenvector corresponding to the largest eigenvalue of $\mathbf{P}_1 \mathbf{P}_2$. In a similar method, we can obtain the SVs of all signals corresponding to the virtual ULA.

3.2 Covariance matrix reconstruction

By using the estimated SVs of all signals $\hat{\mathbf{a}}_j, j = 1, 2, \dots, Q$, we proposed an efficient approach to reconstruct the INCM. The basic concept is to make use of the covariance matrix corresponding to virtual ULA, to estimate the power of the signals and noise. Then, the maximum correlation principle is used to transfer the SVs of the signals associated with the virtual array to the one corresponding to the physical sensors. Finally, by using the estimated SVs and the power of all signals and the noise power, a more accurate INCM is reconstructed.

It is well known that it cannot obtain a good power estimation by using Capon spectrum directly [32]. We take one-signal scenario for example. The covariance matrix of the virtual array is written as

$$\tilde{\mathbf{R}} = \sigma_1^2 \tilde{\mathbf{a}}(\theta_1) \tilde{\mathbf{a}}^H(\theta_1) + \sigma_n^2 \mathbf{I}_{M_\xi+1}. \quad (20)$$

Then, the matrix inversion lemma is used to obtain $\tilde{\mathbf{R}}^{-1}$ as

$$\tilde{\mathbf{R}}^{-1} = \frac{1}{\sigma_n^2} \mathbf{I}_{M_\xi+1} - \frac{\sigma_1^2 \tilde{\mathbf{a}}(\theta_1) \tilde{\mathbf{a}}^H(\theta_1)}{\sigma_n^2 [\sigma_n^2 + (M_\xi + 1) \sigma_1^2]}. \quad (21)$$

Therefore, by using Capon spectrum, the estimated power of the signal is expressed as

$$\hat{\sigma}_1^2 = \frac{1}{\tilde{\mathbf{a}}^H(\theta_1) \tilde{\mathbf{R}}^{-1} \tilde{\mathbf{a}}(\theta_1)} = \sigma_1^2 + \frac{1}{M_\xi + 1} \sigma_n^2. \quad (22)$$

Obviously, the estimated signal power includes the deviation term, i.e. $1/(M_\xi + 1)\sigma_n^2$. Particularly, the estimation performance of power will degrade with the decrease of SNR.

Therefore, according to the modified version of Capon power estimation method in [13] [34] and the eigen-decomposition expression (10), the estimated SVs of signals are used to obtain the power of the j th signal by

$$\hat{\sigma}_j^2 = \frac{1}{\hat{\mathbf{a}}_j^H \mathbf{E}_s \Lambda_s^{-1} \mathbf{E}_s^H \hat{\mathbf{a}}_j}, \quad j = 2, 3, \dots, Q, \quad (23)$$

which can reduce the effect of noise and hence provide a more precise power estimation. By using equation (10), the noise power $\hat{\sigma}_n^2$ is estimated by

$$\hat{\sigma}_n^2 = \frac{1}{M_\xi + 1 - Q} \sum_{q=Q+1}^{M_\xi+1} \lambda_q. \quad (24)$$

It is noted that the INCM cannot be directly reconstructed as

$$\hat{\mathbf{R}}_{i+n} = \sum_{j=2}^Q \hat{\sigma}_j^2 \hat{\mathbf{a}}_j \hat{\mathbf{a}}_j^H + \hat{\sigma}_n^2 \mathbf{I}_{M_\xi+1}, \quad (25)$$

since we cannot implement beamforming in the virtual array. In order to reconstruct the INCM on the actual physical array, we first convert $\hat{\mathbf{a}}_j \in C^{(M_\xi+1) \times 1}$ into the SV corresponding to real physical array as $\mathbf{a}(\theta_j) \in C^{(M+N-1) \times 1}$. Because of the different structure between the estimated $\hat{\mathbf{a}}_j \in C^{(M_\xi+1) \times 1}$ in (19) and $\mathbf{a}(\theta_j)$ in (7), we first resort to the maximum correlation principle [14] [15] to obtain $\mathbf{a}(\theta_j)$. The correlation coefficient of two vectors \mathbf{x}_1 and \mathbf{x}_2 is defined as $\text{cor}(\mathbf{x}_1, \mathbf{x}_2) = (\mathbf{x}_1^H \mathbf{x}_2) / (\|\mathbf{x}_1\| \|\mathbf{x}_2\|)$. For the j th signal, within Θ_j we search a vector $\tilde{\mathbf{a}}_d(\theta_j) \in C^{(M_\xi+1) \times 1}$ with the same vector structure of $\mathbf{a}(\theta_j)$. The expression is written as

$$\begin{aligned} \max_{\tilde{\mathbf{a}}_d(\theta_j)} |\text{cor}(\tilde{\mathbf{a}}_d(\theta_j), \hat{\mathbf{a}}_j)| &= \max_{\tilde{\mathbf{a}}_d(\theta_j)} \frac{|\tilde{\mathbf{a}}_d^H(\theta_j) \hat{\mathbf{a}}_j|}{\|\tilde{\mathbf{a}}_d(\theta_j)\| \|\hat{\mathbf{a}}_j\|} \\ \text{subject to } \theta_j &\in \Theta_j \quad j = 1, 2, \dots, Q \end{aligned} \quad (26)$$

Then, based on the physical array, the SV of j th signal $\mathbf{a}(\theta_j)$ is obtained by using the manifold relationship between $\mathbf{a}(\theta_j)$ and $\tilde{\mathbf{a}}_d(\theta_j)$. In a similar approach, after obtaining the power and the SV information of all signals, the INCM associated with the physical array is reconstructed as

$$\hat{\mathbf{R}}_{i+n} = \sum_{j=2}^Q \hat{\sigma}_j^2 \mathbf{a}(\theta_j) \mathbf{a}^H(\theta_j) + \hat{\sigma}_n^2 \mathbf{I}_{M+N-1}. \quad (27)$$

3.3 Beamformer design

By using the estimated INCM (24) and the DS SV $\mathbf{a}(\theta_1)$ (23), the weight vector of the adaptive beamformer $\mathbf{w}_{\text{proposed}}$ is obtained as

$$\mathbf{w}_{\text{proposed}} = \frac{\hat{\mathbf{R}}_{i+n}^{-1} \mathbf{a}(\theta_1)}{\mathbf{a}^H(\theta_1) \hat{\mathbf{R}}_{i+n}^{-1} \mathbf{a}(\theta_1)}. \quad (28)$$

For clarity, the implementation of the proposed robust adaptive beamforming algorithm is summarized as follows.

1. Preprocess the received covariance matrix of coprime array $\hat{\mathbf{R}}$ (6) and construct the covariance matrix of the virtual array \mathbf{R}_1 using (9).
2. After eigen-decomposing \mathbf{R}_1 and \mathbf{C}_j as described in (10) (15), obtain the matrix \mathbf{P}_1 and \mathbf{P}_2 using (17).
3. Calculate the SVs of all signals and the power of interference signals corresponding to the virtual ULA, respectively using (19) and (23).
4. Obtain the SVs of all signals associated with the physical array using (26).
5. Calculate noise power using (24) and reconstruct INCM $\hat{\mathbf{R}}_{i+n}$ by using (27).
6. Calculate the weight vector of the adaptive beamformer $\mathbf{w}_{\text{proposed}}$ (28).

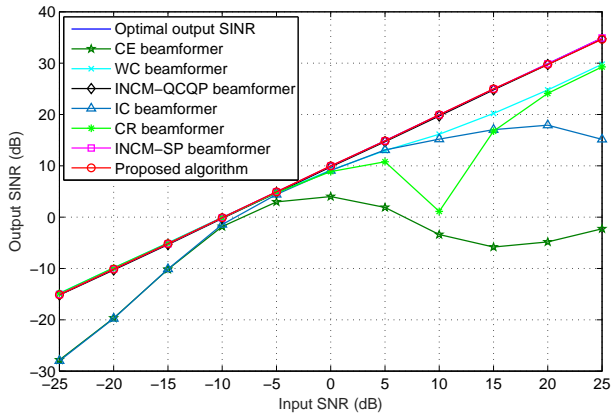
The computational cost of the proposed algorithm is dominated by the eigendecomposition operation in (10), (15) and (19), all of which require $O((M_\xi + 1)^3)$. While the computational load of [13] [15] [16] [33] is $O((M + N - 1)^3)$. That is to say that, compared with other subspace-based approaches, the proposed algorithm has a higher computational complexity. However, since it makes use of virtual array aperture of coprime array, the proposed method can provide more accurate estimations for the signal SV and the power, resulting in a more exact INCM reconstruction. As a result, the proposed algorithm can achieve a better performance than the methods being compared, as we will show through simulation results in the following section.

4 Simulation results

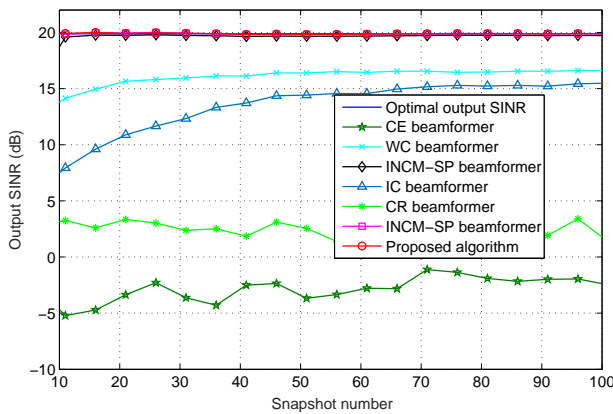
In this section, let us consider a coprime array with a pair of coprime integers $M = 3$ and $N = 5$. The sensor positions of the two sparse subarrays are $[0, 3, 6, 9, 12]d$ and $[0, 5, 10, 15, 20, 25]d$, respectively, and both subarrays share the same reference position. That is to say, there are 10 identical omnidirectional sensors to deploy the coprime array. The unit element spacing d is half-wavelength. Assume that one DS and two interference signals impinge on the coprime array from the directions of $\theta_1 = 0^\circ$, $\theta_2 = 32.5^\circ$ and $\theta_3 = -32.5^\circ$, respectively. Accordingly, The angle sectors of DS and interference signals are $\Theta_1 = [\theta_1 - 4^\circ, \theta_1 + 4^\circ]$, $\Theta_2 = [\theta_2 - 4^\circ, \theta_2 + 4^\circ]$ and $\Theta_3 = [\theta_3 - 4^\circ, \theta_3 + 4^\circ]$, respectively. The additive noise model is a complex circularly symmetric zero-mean white Gaussian random process. The INRs of two interference are 10dB. For each simulation point, 50 Monte Carlo runs are performed.

For performance comparison, since the proposed algorithm is an improved version of the INCM-based subspace projection (SP) (INCM-SP) beamformer [16], we will compare with it in detail. Besides, the conventional eigenspace (CE) beamformer [33], the worst case (WC) beamformer [5], the INCM-based quadratically constrained quadratic programming (INCM-QCQP) beamformer [11], the interference cancellation (IC) beamformer [13], and the correlation reconstruction (CR) beamformer [15] are also presented. The number of signals is assumed to be correctly estimated for subspace-based methods. For the worst case beamformer, the uncertainty parameter is set as $\epsilon = 0.2 \times (M + N - 1)$. In order to ensure a fair comparison, for each compared method, all parameters are chosen to achieve the best performance.

Example 1 : Exactly known signal SVs: In this example, we consider the scenario that the SVs of the DS and the interference signals are



(a) Output SINR versus input SNR

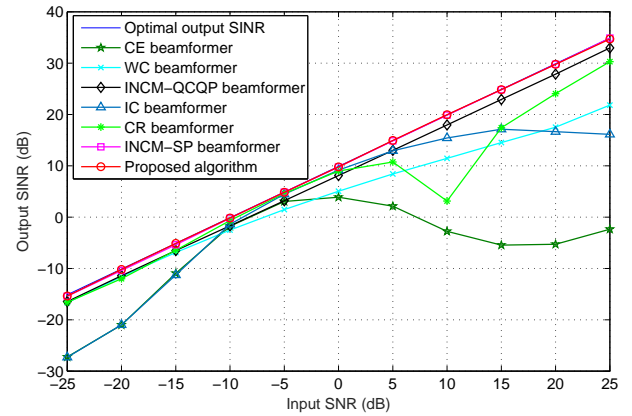


(b) Output SINR versus snapshots

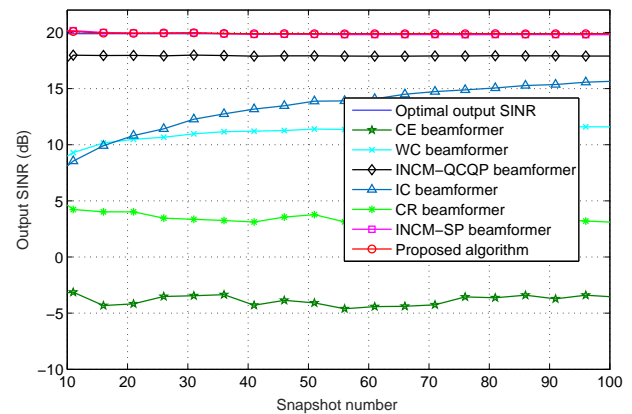
Fig. 1: Output SINR in case of known look direction with 2 interference signals

exactly known. The output SINRs of all methods versus the input SNR are presented in Fig. 1(a), where the number of snapshots is 100. From Fig. 1(a), it is observed that the proposed algorithm, INCM-SP and INCM-QCQP have nearly the same output SINRs, and are superior to CE, WC, IC and CR. Overall, the reconstruction-based approaches outperform the non-reconstruction-based ones. It is also noted that, with known SV information, the proposed algorithm, INCM-SP and INCM-QCQP can approach the optimal output SINR, while CE, WC, IC and CR cannot keep near-optimal performance with the increase of input SNR. The reason is explained that the non-reconstruction-based approaches directly use SCM to design adaptive beamformer. However, SCM contains DS component, which could make the beamformer to suppress DS instead of enhancing it, especially in high SINR case. Fig. 1(b) depicts the output SINR of each method versus snapshot numbers, where the input SNR is 10 dB. In Fig. 1(b), it is shown that the proposed algorithm, INCM-SP and INCM-QCQP not only have faster convergence speeds, but also larger output SINRs than other methods. Furthermore, we find that among reconstruction-based approaches, the proposed algorithm and INCM-SP have a similar convergence performance and approach the optimal SINR.

Example 2 : Fixed signal SV mismatch: Look direction mismatch will degrade beamformer performance. In this example, we consider the case that there is a direction mismatch between assumed look direction of DS and actual one. In detail, the actual look directions of DS and interferences are $\theta_1 = 0^\circ$, $\theta_2 = 32.5^\circ$ and $\theta_3 = -32.5^\circ$, respectively. Whereas we assume them as $\hat{\theta}_1 = 4^\circ$, $\hat{\theta}_2 = 36.5^\circ$ and $\hat{\theta}_3 = -36.5^\circ$, respectively. That is to say, there is a 4° look direction



(a) Output SINR versus input SNR

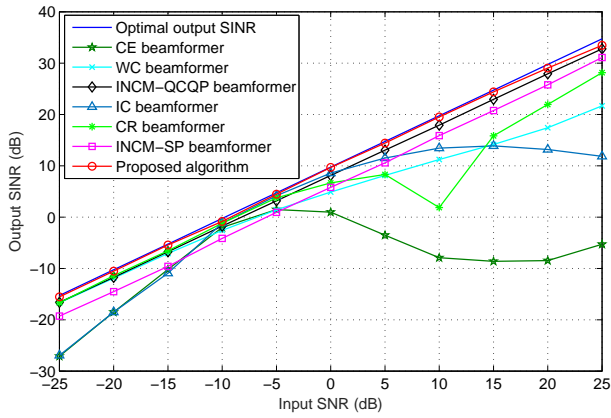


(b) Output SINR versus snapshots

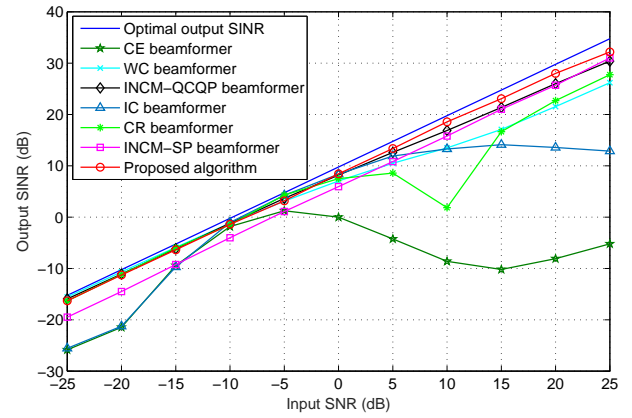
Fig. 2: Output SINR in case of fixed look direction mismatch with 2 interference signals

mismatch for each signal. The output SINR curves for all methods versus input SNR are shown in Fig. 2(a). In Fig. 2(a), it is seen that, similar to Fig. 1(a), the proposed algorithm has almost the same output SINRs as INCM-SP and is very close to the theoretical optimal SINR. It is also observed that the proposed algorithm outperforms INCM-QCQP, CE, WC, IC and CR beamformers. Furthermore, it is seen that, due to the signal SV mismatch, CE and IC exhibit performance degradation in both low and high SNR regions. Fig. 2(b) depicts the output SINRs of the proposed and the other algorithms versus the number of snapshots. As observed from Fig. 2(b), the proposed algorithm presents a faster convergence speed and a higher output SINR than all other beamformers. Similar to Fig. 1(b), the proposed algorithm and INCM-SP have nearly overlapping output SINR as the optimal value. The performance difference between the proposed algorithm and INCM-SP will be shown in the next example.

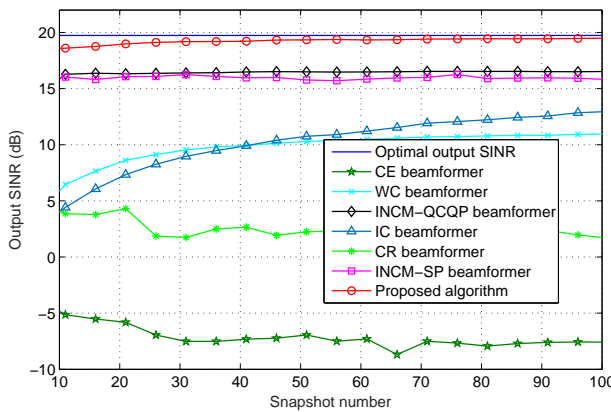
Example 3 : Increased interference number with fixed look direction mismatch: In this example, we add two more interferers with 10dB input INR from the directions of $\theta_4 = 65^\circ$ and $\theta_5 = -65^\circ$, respectively, and their directions are assumed as $\hat{\theta}_4 = 61^\circ$ and $\hat{\theta}_5 = -61^\circ$, respectively. Accordingly, their angle sectors are $\Theta_4 = [\theta_4 - 4^\circ, \hat{\theta}_4 + 4^\circ]$ and $\Theta_5 = [\hat{\theta}_5 - 4^\circ, \theta_5 + 4^\circ]$, respectively. Other simulation settings are identical with Example 2. From Fig. 3(a), it is seen that, to some degree, the performance of all methods degrades because of the increased number of interferers. It is also observed in Fig. 3(a) that the proposed algorithm has the best output SINR performance among all methods and approaches the optimal value similar to Example 1 and Example 2. This is due to the fact that



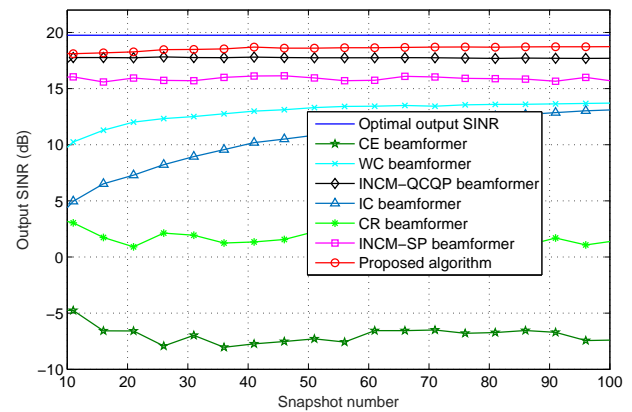
(a) Output SINR versus input SNR



(a) Output SINR versus input SNR



(b) Output SINR versus snapshots



(b) Output SINR versus snapshots

Fig. 3: Output SINR in case of fixed look direction mismatch with 4 interference signals

Fig. 4: Output SINR in case of random look direction mismatch with 4 interference signals

the proposed algorithm takes advantage of the virtual array aperture which equivalently increases the number of sensors, thus obtaining a higher angle resolution. Fig. 3(a) illustrates that the proposed algorithm has a better performance than other methods in terms of the output SINR and the convergence speed.

Example 4 : Random signal direction mismatch: In this example, we assume that DS has a random look direction mismatch. More specifically, the look direction mismatch of the DS is randomly distributed in $[-4^\circ, 4^\circ]$. Other simulation settings are identical to the last example. Note that the look directions of all signals change from trial to trial but keep fixed from snapshot to snapshot. In Fig. 4(a), it is observed that, similar to the previous example, the proposed algorithm still outperforms other methods due to its ability to estimate the SVs of DS and interference signals more accurately than other beamformers. As compared to other eigenspace-based methods, CE and IC present a worse performance. CR has an SINR drop when the input SNR is close to the INR. INCM-SP is sensitive to the number of interferers and there is a performance degradation with interference number increases. The proposed algorithm can achieve a better performance in both low and high input SNR regions. The input SINRs of all approaches versus snapshots are shown in Fig. 4(b). It is seen that, clearly, the proposed algorithm can converge to the steady-state fast and achieves a near-optimal SINR performance. Therefore, the proposed algorithm has a better robustness under the condition where the look directions of signals have a random mismatch.

5 Conclusion

A novel robust adaptive beamforming algorithm is proposed for coprime array in this paper. According to the projection method, the actual SVs of the DS and the interference signals are estimated from an intersection of two subspaces. Moreover, their power is obtained by using the covariance fitting approach. Then, the maximum correlation principle is used to reconstruct the INCM based on the physical array rather than the virtual one. Since coprime array has a larger array aperture than ULA with the same number of physical sensors, the proposed algorithm can obtain more accurate estimation for DOAs and power of signals, leading to a more precise INCM reconstruction. Finally, with the estimated DS SV and INCM, the proposed adaptive beamformer is formulated in accordance with the MVDR criterion. Simulation results clearly demonstrate that the proposed algorithm provides a better performance than existing subspace-based adaptive beamformers.

6 Acknowledgments

The work of K. Liu was supported by the China Scholarship Council for his stay at the Temple University. The work of Y.D. Zhang was supported in part by the National Science Foundation under Grant No. AST-1547420.

7 References

- 1 Vorobyov, S. A.: 'Principles of minimum variance robust adaptive beamforming design', *Signal Process.*, 2013, **93**, (12), pp. 3264-3277
- 2 Gershman, A. B., Sidiropoulos, N. D., Shahbazpanahi, S., *et al.*: 'Convex optimization-based beamforming', *IEEE Signal Process. Mag.*, 2010, **27**,(3), pp. 62-75
- 3 Qian, H., Liu, K., and Wang, W.: 'Shrinkage widely linear recursive least square algorithms for beamforming', *IEICE Trans. Commun.*, 2016, **99**, (7), pp. 1532-1540
- 4 Capon, J.: 'High-resolution frequency-wavenumber spectrum analysis', *Proc. IEEE*, 1969, **57**, (8), pp. 1408-1418
- 5 Vorobyov, S. A., Gershman, A. B., and Luo, Z.: 'Robust adaptive beamforming using worst-case performance optimization: A solution to the signal mismatch problem', *IEEE Trans. Signal Process.*, 2003, **51**, (2), pp. 313-324
- 6 Hassanien, A., Vorobyov, S. A., and Wong, K.: 'Robust adaptive beamforming using sequential quadratic programming: An iterative solution to the mismatch problem', *IEEE Signal Process. Lett.*, 2008, **15**, pp. 733-736
- 7 Khabbazibasmenj, A., Vorobyov, S. A., and Hassanien, A.: 'Robust adaptive beamforming based on steering vector estimation with as little as possible prior information', *IEEE Trans. Signal Process.*, 2012, **60**, (6), pp. 2974-2987
- 8 Li, J., Stoica, P., and Wang, Z. S.: 'On robust Capon beamforming and diagonal loading', *IEEE Trans. Signal Process.*, 2003, **51**, (7), pp. 1702-1715
- 9 Du, L., Li, J., and Stoica, P.: 'Fully automatic computation of diagonal loading levels for robust adaptive beamforming', *IEEE Trans. Aerosp. Electron. Syst.*, 2010, **46**, (1), pp. 449-458
- 10 Gu, Y., and Leshem, A.: 'Robust adaptive beamforming based on jointly estimating covariance matrix and steering vector'. Proc. IEEE Int. Conf. Acoustics, Speech, and Signal Processing (ICASSP), Prague, Czech Republic, May 2011, pp. 2640-2644
- 11 Gu, Y., and Leshem, A.: 'Robust adaptive beamforming based on interference covariance matrix reconstruction and steering vector estimation', *IEEE Trans. Signal Process.*, 2012, **60**, (7), pp. 3881-3885
- 12 Gu, Y., Goodman, N. A., Hong, S., *et al.*: 'Robust adaptive beamforming based on interference covariance matrix sparse reconstruction', *Signal Process.*, 2014, **96**, pp. 375-381
- 13 Zhuang, J., and Manikas, A.: 'Interference cancellation beamforming robust to pointing errors', *IET Signal Process.*, 2013, **7**, (2), pp. 120-127
- 14 Shen, F., Chen, F., and Song, J.: 'Robust adaptive beamforming using low-complexity correlation coefficient calculation algorithms', *Electron. Lett.*, 2015, **51**, (6), pp. 443-445
- 15 Shen, F., Chen, F., and Song, J.: 'Robust adaptive beamforming based on steering vector estimation and covariance matrix reconstruction', *IEEE Commun. Lett.*, 2015, **19**, (9), pp. 1636-1639
- 16 Yuan, X., and Gan, L.: 'Robust adaptive beamforming via a novel subspace method for interference covariance matrix reconstruction', *Signal Process.*, 2017, **130**, pp. 233-242
- 17 Vaidyanathan, P. P., and Pal, P.: 'Sparse sensing with co-prime samplers and arrays', *IEEE Trans. Signal Process.*, 2011, **59**, (2), pp. 573-586
- 18 Wang, M., and Nehorai, A.: 'Coarrays, MUSIC, and the Cramer-Rao Bound', *IEEE Trans. Signal Process.*, 2016, **65**, (4), pp. 933-946
- 19 Zhang, Y. D., Amin, M. G., and Himed, B.: 'Sparsity-based DOA estimation using co-prime arrays'. Proc. IEEE Int. Conf. Acoustics, Speech, and Signal Processing (ICASSP), Vancouver, Canada, May 2013, pp. 3967-3971
- 20 Qin, S., Zhang, Y. D., and Amin, M. G.: 'Generalized coprime array configurations for direction-of-arrival estimation', *IEEE Trans. Signal Process.*, 2015, **63**, (6), pp. 1377-1390
- 21 Zhou, C., Gu, Y., Zhang, Y. D., *et al.*: 'Compressive sensing based coprime array direction-of-arrival estimation', *IET Commun.*, 2017, **11**, (11), pp. 1719-1724
- 22 Qin, S., Zhang, Y. D., Amin, M. G., *et al.*: 'Generalized Coprime Sampling of Toeplitz Matrices for Spectrum Estimation', *IEEE Trans. Signal Process.*, 2017, **65**, (1), pp. 81-94
- 23 Ahmed, A., Zhang, Y. D., and Himed, B.: 'Effective nested array design for fourth-order cumulant-based DOA estimation'. in Proc. IEEE Radar Conf., Seattle, WA, USA, May 2017, pp. 0998-1002
- 24 Gu, Y., Zhou, C., Goodman, N. A., *et al.*: 'Coprime array adaptive beamforming based on compressive sensing virtual array signal'. in Proc. IEEE Int. Conf. Acoust., Speech, Signal Process. (ICASSP), Shanghai, China, Mar. 2016, pp. 2981-2985
- 25 Zhou, C., Shi, Z., and Gu, Y.: 'Coprime array adaptive beamforming with enhanced degrees-of-freedom capability'. in Proc. IEEE Radar Conf., Seattle, WA, USA, May 2017, pp. 1357-1361
- 26 Zhou, C., Gu, Y., Song, W. Z., *et al.*: 'Robust adaptive beamforming based on DOA support using decomposed coprime sub-arrays'. in Proc. IEEE Int. Conf. Acoust., Speech, Signal Process. (ICASSP), Shanghai, China, Mar. 2016, pp. 2986-2990
- 27 Zhou, C., Gu, Y., He, S., *et al.*: 'A robust and efficient algorithm for coprime array adaptive beamforming', *IEEE Trans. Veh. Technol.*, 2018, **67**, (2), pp. 1099-1112
- 28 Shi, Z., Zhou, C., Gu, Y., *et al.*: 'Source estimation using coprime array: A sparse reconstruction perspective', *IEEE Sensors J.*, 2017, **17**, (3), pp. 755-765.
- 29 Liu, C., and Vaidyanathan, P. P.: 'Remarks on the spatial smoothing step in coarray MUSIC', *IEEE Signal Process. Lett.*, 2015, **22**, (9), pp. 1438-1442
- 30 Huang, F., Sheng, W., and Ma, X.: 'Modified projection approach for robust adaptive array beamforming', *Signal Process.*, 2012, **92**, (7), pp. 1758-1763
- 31 Zhang, F., and Zhang, Q.: 'Eigenvalue inequalities for matrix product', *IEEE Trans. Autom. Control.* 2006, **51**, (9), pp. 1506-1509
- 32 Li, J., Stoica, P., and Wang, Z.: 'On robust Capon beamforming and diagonal loading', *IEEE Trans. Signal Process.*, 2003, **51**, (7), pp. 1702-1715
- 33 Chang, L., and Yeh, C. C.: 'Performance of DMI and eigenspace-based beamformers', *IEEE Trans. Antennas Propag.*, 1992, **40**, (11), pp. 1336-1347
- 34 McCloud, M. L., Scharf, L. L.: 'A new subspace identification algorithm for high-resolution DOA estimation', *IEEE Trans. Antennas Propag.*, 2002, **50**, (10), pp. 1382-1390